Anal. Chem. **2004,** *76,* 4741−4746

Nuclear Localization of Aminoacyl-tRNA Synthetases Using Single-Cell Capillary Electrophoresis Laser-Induced Fluorescence Analysis

Nilhan Gunasekera,[†,§] Sang Won Lee,[‡] Sunghoon Kim,[‡] Karin Musier-Forsyth,[†] and Edgar Arriaga*[,†]

Department of Chemistry, University of Minnesota, 207 Pleasant Street SE, Minneapolis, Minnesota 55455, and National Creative Research Initiatives Center for ARS Network College of Pharmacy, Seoul National University San 56-1, Shillim-dong, Kwanak-gu, Seoul 151-746, Korea

Aminoacyl-tRNA synthetases (aaRSs) are a family of enzymes whose function in specific aminoacylation of tRNAs is central to the process of protein translation, which occurs in the cytoplasm of all living cells. In addition to their well-established cytoplasmic localization, fluorescence microscopy studies and analysis of the aminoacylation state of nuclear tRNAs have revealed that synthetases are localized in the nuclei of cells from several species including *Xenopus laevis* and *Saccharomyces cerevisiae*. Whether nuclear localization of aaRSs is a general phenomenon that occurs in all eukaryotic cells is an open question. In the work described here, human methionyl-tRNA synthetase (MRS) and human lysyl-tRNA synthetase (KRS) were expressed in human-derived ΔH2-1 osteosarcoma cells as enhanced green fluorescent protein (EGFP) fusion proteins. The subcellular localization of these EGFP-aaRSs was first probed by fluorescence microscopy using cells that coexpressed EGFP-aaRS and a nuclear marker fusion protein, nuDsRed. As expected, both aaRSs were present in the cytosol, while only EGFP-MRS was also clearly localized in the nucleus. To confirm these findings, and to investigate a potentially more sensitive, general method for nuclear localization studies, capillary electrophoresis with laser-induced fluorescence (CE-LIF) detection was used to analyze single ΔH2-1 cells expressing both EGFP-aaRS and nuDsRed. While cytosolic EGFP signals were detected for both EGFP-MRS and EGFP-KRS, only EGFP-MRS was found in the nucleus, along with nuDsRed. The detection of EGFP-MRS in nuclei of ΔH2-1 cells demonstrates the feasibility of using CE-LIF analysis in nuclear localization studies of proteins in mammalian cells.

Aminoacyl-tRNA synthetases (aaRSs) catalyze a two-step reaction known as aminoacylation, wherein a specific amino acid is activated with ATP and subsequently transferred to its cognate tRNA. It has been shown that protein synthesis is highly compartmentalized in higher eukaryotes.[1] This organization facilitates channeling of aminoacyl-tRNAs from the aaRS to the ribosomes, which are the site of protein synthesis in the cytoplasm. It is not surprising that the majority of aaRSs are also localized in the cytoplasm.[1−6] However, the presence of a minor fraction of aaRSs in the nuclei of certain cells has also been reported.[3,4,7−14] In recent years, studies demonstrating tRNA aminoacylation within the nucleus have been used as indirect evidence for the nuclear localization of aaRSs from *Xenopus laevis* oocytes.[11] Since prevention of tRNA aminoacylation prevented nuclear export, nuclear tRNA aminoacylation has been proposed to function as a proofreading step that monitors tRNA processing prior to export.[11] The localization of aaRSs in the nuclei of *Saccharomyces cerevisiae* was predicted by sequence analysis of the yeast cytosolic aaRS database, which resulted in the identification of several putative nuclear localization signals (NLSs).[15] Indeed, aminoacylation of tRNAs in the nucleus of *S. cerevisiae* has been observed,[10] and functional pools of tyrosyl-tRNA synthetase have been found in the nuclei of budding yeast.[14] In higher

* Corresponding author. Phone: 612-624-8024. Fax: 612-626-7541. E-mail: arriaga@chem.umn.edu.

† University of Minnesota.

§ Present address: University of Wisconsin, 518 South 7th Avenue, Wausau, WI 54401.

‡ Seoul National University.

(1) Kisselev, L. L.; Wolfson, A. D. *Prog. Nucleic Acid Res. Mol. Biol.* **1994**, *48*, 83−142.
(2) Dimitrijevic, L. *FEBS Lett.* **1977**, *79*, 37−41.
(3) Barbarese, E.; Koppel, D. E.; Deutscher, M. P.; Smith, C. L.; Ainger, K.; Morgan, F.; Carson, J. H. *J. Cell Sci.* **1995**, *108* (Part 8), 2781−2790.
(4) Nathanson, L.; Deutscher, M. P. *J. Biol. Chem.* **2000**, *275* (41), 31559−31562.
(5) Agris, P. F.; Woolverton, D. K.; Setzer, D. *Proc. Natl. Acad. Sci. U.S.A.* **1976**, *73*, 3857−3861.
(6) Nathanson, L.; Xia, T.; Deutscher, M. P. *RNA* **2003**, *9*, 9−13.
(7) Galani, K.; Grosshans, H.; Deinert, K.; Hurt, E. C.; Simos, G. *EMBO J.* **2001**, *20*, 6889−6898.
(8) Vazquez-Abad, D.; Carson, J. H.; Rothfield, N. *Cell Tissue Res.* **1996**, *286*, 487−491.
(9) Ko, Y. G.; Kang, Y. S.; Kim, E. K.; Park, S. G.; Kim, S. *J. Cell Biol.* **2000**, *149*, 567−574.
(10) Sarkar, S.; Azad, A. K.; Hopper, A. K. *Proc. Natl. Acad. Sci. U.S.A.* **1999**, *96*, 14366−14371.
(11) Lund, E.; Dahlberg, J. E. *Science* **1998**, *282*, 2082−2085.
(12) Popenko, V. I.; Ivanova, J. L.; Cherny, N. E.; Filonenko, V. V.; Beresten, S. F.; Wolfson, A. D.; Kisselev, L. L. *Eur. J. Cell Biol.* **1994**, *65*, 60−69.
(13) Grosshans, H.; Hurt, E.; Simos, G. *Genes Dev.* **2000**, *14*, 830−840.
(14) Azad, A. K.; Stanford, D. R.; Sarkar, S.; Hopper, A. K. *Mol. Biol. Cell* **2001**, *12*, 1381−1392.
(15) Schimmel, P.; Wang, C. C. *Trends Biochem. Sci.* **1999**, *24*, 127−128.

10.1021/ac049567e CCC: $27.50
Published on Web 07/20/2004

eukaryotes, at least nine aaRSs are part of a high molecular weight multi-enzyme complex,[1,16−18] and the presence of active aaRSs in nuclei of two different mammalian cell lines has been reported.[4] Interestingly, the nuclear aaRSs appear to be organized into a complex that is even more stable than the cytoplasmic complex.

In addition to the aminoacylation activity studies described above, microscopy has previously been used to more directly visualize nuclear pools of aaRSs in mammalian cells. For example, confocal microscopy was used to localize immuno-labeled histidyl-tRNA synthetase to the cytosol and nucleus of a human laryngeal cell line.[8] Another study using fluorescence in situ hybridization (FISH) and confocal microscopy found that arginyl-tRNA synthetase is present in nuclei of mouse oligodendrocytes.[3]

Several putative functions have been ascribed to nuclear aaRSs including involvement in the final proofreading of tRNAs prior to export as mentioned above,[11] a role in the biogenesis of rRNA in nucleoli,[9] and even participation in nuclear protein synthesis.[19] Although numerous studies examining nuclear localization of aaRSs have been reported, most of the methods used are indirect or the results are ambiguous due to the possibility of cytoplasmic contamination and the lack of a physical separation of subcellular compartments. Thus, there is a need for a more general, sensitive, and efficient method of probing the subcellular localization of proteins such as aaRSs.

Bulk level cell fractionation can be used to physically separate nuclei from cytoplasmic and other subcellular compartments. However, this method often leads to fragmentation of organelles since they are prepared by mechanical disruption of cells.[20] Furthermore, bulk preparations may contain contaminating organelles that can lead to incorrect conclusions regarding the localization of biomolecules.[6,20] Additionally, bulk isolations can also result in enzyme redistribution and activation of unwanted enzyme activity.[21]

Analysis of protein localization using single cells offers several potential advantages over bulk level analyses. In addition to minimizing contamination problems associated with the latter, the ability to perform localization studies on a selected individual cell avoids problems associated with low transfection efficiencies often associated with fusion proteins.[22]

We have recently reported the use of capillary electrophoresis with laser-induced fluorescence (CE-LIF) detection to analyze nuclei from single cells.[23] Briefly, single cells expressing nuDsRed, a nuclear-targeted fusion protein, were injected into a capillary and selectively lysed using digitonin to release their organellar contents, followed by electrophoretic separation. It was demonstrated that nuclear peaks could be identified based on the intensity of the observed signal and the selectivity of nuDsRed for nuclei.

In the work described here, we probe the subcellular localization of enhanced green fluorescent protein (EGFP)-tagged lysyl-tRNA synthetase (EGFP-KRS) and methionyl-tRNA synthetase (EGFP-MRS) in human osteosarcoma cells using CE-LIF-based single-cell analysis. We chose MRS, in part, because it has previously been localized in the nucleus of *S. cerevisiae*,[7] *X. laevis*,[11] and Hela cells.[9] The latter study involved direct visualization of MRS in the nucleolus of proliferative cells using confocal immunofluorescence microscopy. In contrast, although KRS activity has been detected in nuclei of mammalian cells,[4] direct visualization of nuclear KRS has not yet been reported.

EXPERIMENTAL PROCEDURES

Chemicals. Tris[hydroxymethyl]aminomethane (Tris), (*N*-[2-hydroxyethyl]piperazine-*N*-ethanesulfonic acid]) (HEPES), phosphate-buffered saline (PBS), Dulbecco's modified Eagle's medium, and calf serum were from Sigma (St. Louis, MO). Trypan blue stain was purchased from BioWhitaker (Walkersville, MD), and fluorescein was from Molecular Probes (Eugene, OR).

Cell Culture. ΔH2-1 cells (a kind gift from Dr. Carlos Moraes, Department of Neurology and Cell Biology & Anatomy, University of Miami, FL) were cultured at 37 °C and 5% CO_2 by splitting cells 1:6 every 3−4 days in modified Eagle's medium supplemented with 10% fetal bovine serum. NS1 cells were maintained similarly, with the exception of using 10% calf serum in the Dulbecco's modified Eagle's medium.

Proteins and Plasmids. Recombinant EGFP was purchased from Clontech (Palo Alto, CA). The nuclear-localized protein nuDsRed was expressed from a commercially available plasmid, pDsRed2Nuc (BD Biosciences, NJ). This plasmid contains the nuclear localization signal from the SVT40 antigen. Plasmids encoding EGFP-KRS and EGFP-MRS were constructed using the pEGFP-C2 vector (Clontech, CA) by fusing the human-derived aaRS gene to the C-terminus of the gene encoding EGFP. Lipofection of these plasmids into mammalian cells was carried out in a 24-well plate according to the manufacturer's instructions using 4−5 μg of plasmid DNA and 3 μL of dimyristyl−rosenthal inhibitor ether lipid C (DMRIE-C) (Life Technologies, MD) per well.

Imaging of Cells and Nuclear Species. Images were collected using a Nikon TE300 fluorescence microscope using a 600× objective lens (Fryer Co. Inc., Huntley, IL). The standard filter settings used were as follows. In the green setting the excitation range was 465−495 nm while the emission range was 515−555 nm. In the red setting the excitation range was 518−552 nm while the emission range was 590−650 nm. Visualization of nuDsRed was performed with the red setting (absorption range is 450−600 nm, maximum at 561 nm; emission range is 550−675 nm, maximum at 587 nm). Visualization of EGFP was performed with the green setting (absorption range is 400−520 nm, maximum at 489 nm; emission range is 500−575 nm, maximum at 508 nm). A CCD camera (Model KX85, Apogee Instruments Inc., Auburn, CA) was used to collect these images. The camera was cooled to 0 °C, and the exposure time was set to 40 ms.

Single-Cell Injection and Disruption. The adherent ΔH2-1 cells were washed with phosphate-buffered saline (PBS), trypsinized (0.5% trypsin) for 5 min, pelleted at 600×*g*, and washed and resuspended in CE buffer A (250 mM sucrose, 10 mM HEPES, pH 7.4). The hydrodynamic siphoning injection method has been described elsewhere.[24,25] Briefly, a droplet of cell culture is deposited onto a microscope slide and a capillary is positioned

(16) Bandyopadhyay, A. K.; Deutscher, M. P. *J. Mol. Biol.* **1971**, *60*, 113−122.
(17) Mirande, M. *Prog. Nucleic Acid Res. Mol. Biol.* **1991**, *40*, 95−142.
(18) Yang, D. C. *Curr. Top. Cell. Regul.* **1996**, *34*, 101−136.
(19) Dahlberg, J. E.; Lund, E.; Goodwin, E. B. *RNA* **2003**, *9*, 1−8.
(20) Gunasekera, N.; Musier-Forsyth, K.; Arriaga, E. *Electrophoresis* **2002**, *23*, 2110−2116.
(21) Sims, C. E.; Allbritton, N. L. *Curr. Opin. Biotechnol.* **2003**, *14*, 23−28.
(22) von Laer, D.; Lindemann, D.; Roscher, S.; Herwig, U.; Friel, J.; Herchenroder, O. *Virology* **2001**, *288*, 139−144.
(23) Gunasekera, N.; Olson, K. J.; Musier-Forsyth, K.; Arriaga, E. A. *Anal. Chem.* **2004**, *76*, 655−662.

with its axis perpendicular to the microscope slide surface. A successfully transfected, fluorescing cell is selected and injected into the capillary by positioning the injection end of the capillary within a few micrometers directly above the cell and by creating a pressure difference (11 kPa for 1 s) between the injection and detection ends of the capillary. Once the cell has been injected, a plug of digitonin (1 mg/mL in buffer A) is electrokinetically (400 V/cm, 5 s) injected to selectively disrupt the plasma membrane. After the detergent has been injected, the injection end of the capillary is inserted into a vial containing buffer A. The cell is incubated in the detergent for a total of 1.5 min. To confirm that the detergent successfully permeabilized the plasma membrane, following cell and detergent injection, the capillary was mounted on a fluorescence microscope and monitored for staining of the nucleus with ethidium homodimer, a plasma membrane impermeant nuclear stain (Molecular Probes, Eugene, OR).

CE Separation and LIF Detection. After incubating single cells with digitonin inside the capillary, electrophoresis was carried out at 400 V/cm for at least 15 min. At the end of each separation, the capillary was reconditioned by pressure flushing using the CE run buffer contained within a syringe fitted to the capillary through an adapter (Valco Instruments Co., Inc., Houston, TX).

The LIF detector and its use have been previously described.[26] For excitation, the 488-nm Ar-ion laser line output was set at 7 mW (model 532-BS-A04, Melles Griot, Carlsbad, CA). All spectral filters used were purchased from Omega Optical Inc. (Brattleboro, VT). Scattering was reduced by using long-pass filters (495 AELP, 505 AELP). The height difference between the sheath-flow buffer meniscus and the detector was 15 cm. EGFP fluorescence was selected with a band-pass filter (535DF35) that selects the fluorescence in the 518−552 nm range (green channel). nuDsRed fluorescence was filtered with a 635DF55 band-pass filter that selects the 612−662 nm range (red channel). The intensity of selected spectral regions was measured with a R1471 photomultiplier tube (Hamamatsu, Bridgewater, NJ). The output of the photomultiplier tube was digitized at 100 Hz using a NiDaq I/O board (PCI-MIO-16XE-50, National Instruments, Austin, TX), and the data were saved as a binary file.

The detector was aligned using a 10^{-9} M solution of fluorescein. Briefly, during a continuous electrokinetic flow of fluorescein at 400 V/cm through the capillary, the position of the sheath-flow cuvette housing the capillary was adjusted until the signal from fluorescein is maximized. The limit of detection for fluorescein was 2.3 zmol. The relative standard deviation for the peak intensity of individual fluorescent microspheres was 23%. Fluorescent species were detected as they migrated out of the capillary by excitation with a 488 nm Ar-ion laser line.

Dual-channel detection was used to simultaneously detect both the green and the red fluorophores (Figure 1). Samples were excited by a 488 nm Ar-ion laser, and the resultant fluorescence was filtered using two long-pass filters (495 AELP and 505AELP) to reduce scatter followed by a pinhole to spatially select filtered light. A dichroic mirror was used to transmit red light (>550 nm) and reflect green light (<550 nm). After spectral separation of the emitted light, fluorescence was further filtered with interference filters, described above for the red and green channels, before reaching separate photomultiplier tubes.

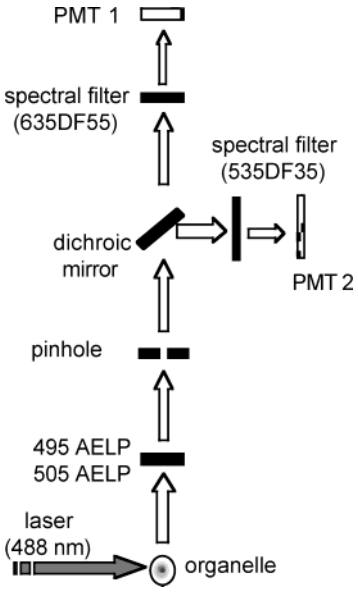

Figure 1. Schematic diagram of CE-dual LIF detection system. A laser excites fluorophores in the sample, and the presence of scatter filters and a pinhole reduce scattering. A dichroic mirror transmitted spectrally split fluorescence into two regions, which are further filtered with spectral filters (535DF35 for EGFP and 635DF55 for nuDsRed). Separate photomultiplier tubes (PMT) monitor fluorescence in each spectral region.

Data Analysis. The procedures for data analysis have been described previously.[26] With the use of an Igor-Pro (Wavemetrics Lake Oswego, OR) algorithm, individual organellar peaks (narrow peaks) can be separated from cytosolic fluorescent species (broad peaks). The molar amount of EGFP-MRS found in the cytosolic and nuclear compartments was determined using a recombinant EGFP as a standard.

RESULTS AND DISCUSSION

Subcellular Localization of EGFP-KRS and EGFP-MRS by Microscopy. EGFP-MRS and EGFP-KRS were chosen as a model system to study the nuclear localization of aaRSs by CE-LIF. Each fusion protein was coexpressed in ΔH2-1 cells along with nuDsRed, a nuclear marker. The resulting fluorescence was initially monitored by microscopy. If the red fluorescence of nuDsRed overlaps with the green fluorescence of EGFP in a cell expressing both these proteins, then it can be concluded that the EGFP-aaRS is localized in the nucleus.

To check whether each of these fluorophores could be selectively detected under the appropriate filter setting, cells expressing only EGFP or only nuDsRed were imaged using both the green and the red filter settings. As shown in Figure 2A (left panels), the EGFP fluorescence was detected only in the green filter setting. Similarly, nuDsRed fluorescence was detected only in the red filter setting (Figure 2A, right panels). Thus, the two fluorophores can be independently detected under the appropriate filter settings using fluorescence microscopy.

Figure 2B shows sample cells from cultures coexpressing nuDsRed with either EGFP-KRS (top panels) or EGFP-MRS

(24) Krylov, S. N.; Arriaga, E. A.; Chan, N. W.; Dovichi, N. J.; Palcic, M. M. *Anal. Biochem*. **2000**, *283*, 133−135.
(25) Anderson, A. B.; Gergen, J.; Arriaga, E. A. *J. Chromatogr., B* **2002**, *769*, 97−106.
(26) Duffy, C. F.; Gafoor, S.; Richards, D. P.; Admadzadeh, H.; O'Kennedy, R.; Arriaga, E. A. *Anal. Chem*. **2001**, *73*, 1855−1861.

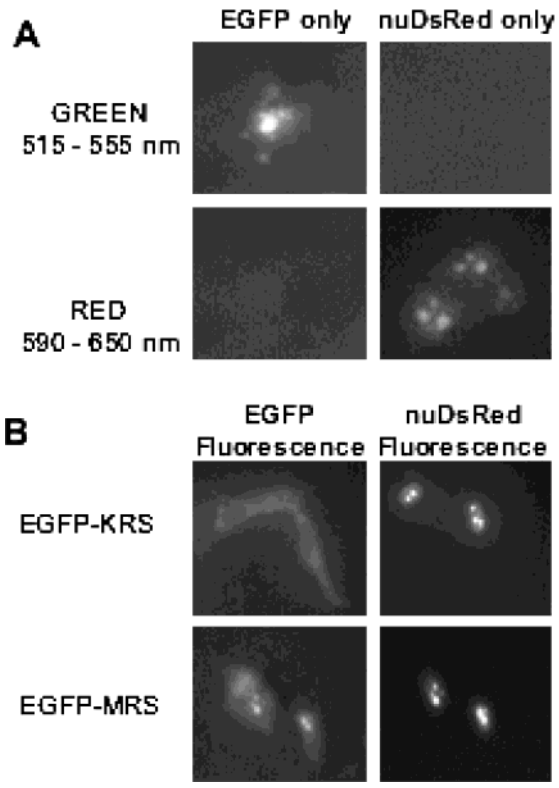

Figure 2. Fluorescence microscopy analysis of cells expressing EGFP and nuDsRed. (A) Cells transfected with pEGFP-KRS only (left panels) or pDsRed2Nuc only (right panels). These cells were observed through a green filter setting (top) or red filter setting (bottom). (B) Cells transfected with both pDsRed2Nuc and pEGFP-KRS (top) or with both pDsRed2Nuc and pEGFP-MRS (bottom). Filter settings were the same as those in panel A. Imaging was carried out 24 h post-transfection. Magnification was 60×. Other conditions are described in the Experimental Procedures section.

(bottom panels). Only the EGFP-MRS cell was clearly observed in the nucleus, while both EGFP-MRS and EGFP-KRS showed cytosolic green fluorescence. Thus, it appears that EGFP-MRS is localized both in the cytosol and the nucleus. This nuclear localization of EGFP-MRS is consistent with previous reports that MRS is present in the nucleus.[7,9]

The presence of a putative nuclear localization signal (PGK-TKKG) beginning at position 188 of the 597-amino acid sequence of human KRS, as well as the prediction by PSORT software,[27] suggests that KRS would also be localized to the nucleus. The failure to clearly detect EGFP-KRS in the nucleus may be due to the inability to separate the nuclear fluorescence from cytosolic fluorescence due to low resolution and high background fluorescence, which are shortcomings of the microscopy technique. Alternatively, fusion of EGFP to the KRS N-terminus may prevent nuclear import.

Cytosolic Localization of EGFP-KRS and EGFP-MRS by CE-LIF. CE-LIF was next used to monitor the subcellular localization of EGFP-MRS and EGFP-KRS in ΔH2-1 cells. Cytosolic EGFP is expected to diffuse appreciably during the CE separation and may adsorb to the capillary walls resulting in a broad peak, whereas EGFP contained within an organelle will not diffuse and should yield a narrow peak.

(27) *PSORT Software*; http://www.psort.nibb.ac.jp.

Figure 3A is an electropherogram from a typical single cell expressing EGFP-MRS. As expected, a broad peak (peak width 20.5 ± 0.3 s, $n = 3$) was observed at approximately 570 s, consistent with the cytosolic localization of EGFP-MRS. In addition to this broad peak, narrow organellar peaks were also detected for EGFP-MRS cells (peak width 88 ± 23 ms, $n = 3$). The width of the narrow peaks corresponds to the time organelles take to travel through the focused laser beam (∼70 μm diameter) used for the excitation source of the postcolumn LIF detector. On the other hand, the width of the broad peaks (e.g., 1.6 cm or 3.6% of the capillary length) clearly indicates that other broadening sources, present during the electrophoretic separation, are dominant.

We confirmed that the broad peak was due to cytosolic EGFP by comparing the signals from cells expressing EGFP-KRS or -MRS with signals from untransfected cells. Figure 3B shows the peak profiles from a cell expressing EGFP-MRS (trace I), EGFP-KRS (trace II), and an untransfected cell (trace III). For clarity, these electropherograms have been processed to show only the broad peaks, as described in the Experimental Procedures section. As expected, the late migrating broad peaks in traces I and II were not detected in the trace from the untransfected cell (trace III). The first peak (193 ± 19 s, $n = 3$) observed in all three traces has been previously identified to be caused by the cell medium.[20,28] The second peak in trace III (304 ± 16 s, $n = 3$) is caused by the detergent used to lyse the cell (data not shown). This peak is not always detected in analysis of cells expressing EGFP (traces I and II) since it is not well resolved from the background in many traces.

In CE, migration time is determined by a combination of factors including size-to-charge ratio and capillary−wall interactions.[29] Therefore, as expected, the migration times for the two different EGFP fusion proteins are somewhat different (compare traces I and II in Figure 3B). The cytosolic EGFP-MRS signal consists of two closely migrating peaks (Figures 3A and 3B, trace I). In some cells the earlier peak is more predominant (Figure 3B, trace I), while in others the later one is larger (Figure 3A). It is possible that these two peaks correspond to different isoforms of this protein.[30]

Detection of Organellar Peaks by CE-LIF. In addition to the broad cytosolic peak, narrow organellar peaks are also detected for EGFP-MRS cells (Figure 3A). Figure 3C contains a set of electropherograms that were processed to show only the narrow peaks, as described in the Experimental Procedures section. Trace I is from a cell expressing only EGFP-MRS, whereas trace II was obtained from a cell expressing only EGFP-KRS, and trace III is from an untransfected cell. We observe an intense narrow signal (1.54 ± 0.91 V, $n = 6$) only in the case of the EGFP-MRS cell (trace I). This signal can be clearly distinguished from the low-intensity peaks (0.16 ± 0.16 V, $n = 8$) detected in untransfected cells (trace III). The narrow peaks observed in the latter are due to low amounts of autofluorescence and scatter. Thus, the intensity and width of the narrow peak in trace I is

(28) Malek, A.; Khaledi, M. G. *Anal. Biochem*. **1999**, *268*, 262−269.
(29) Landers, J.; Oda, R. *Handbook of Capillary Electrophoresis*; CRC Press: Boca Raton, FL, 1997.
(30) Schaumloffel, D.; Prange, A.; Marx, G.; Heumann, K. G.; Bratter, P. *Anal. Bioanal. Chem*. **2002**, *372*, 155−163.

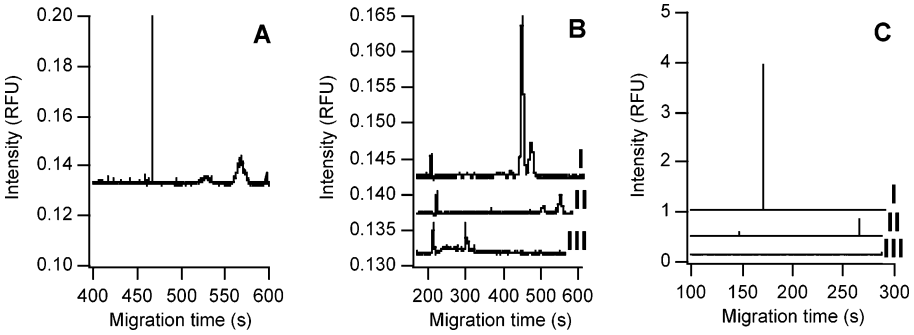

Figure 3. Single-cell CE-LIF analysis. (A) Electropherogram from a single cell expressing only EGFP-MRS showing both broad and narrow peaks. (B) Electropherograms from single cells expressing EGFP-MRS (I), EGFP-KRS (II), and from untransfected cells (III) showing broad events. (C) Electropherogram from single cells expressing EGFP-MRS (I), EGFP-KRS (II), and from untransfected cells (III) showing narrow events. For clarity, traces I and II have been offset on the *y*-axis. Only the green channel was used. The separation was conducted in buffer A at 400 V/cm in a 50 μm i.d. bare fused-silica capillary (44.1 cm). Other conditions are described in the Experimental Procedures section.

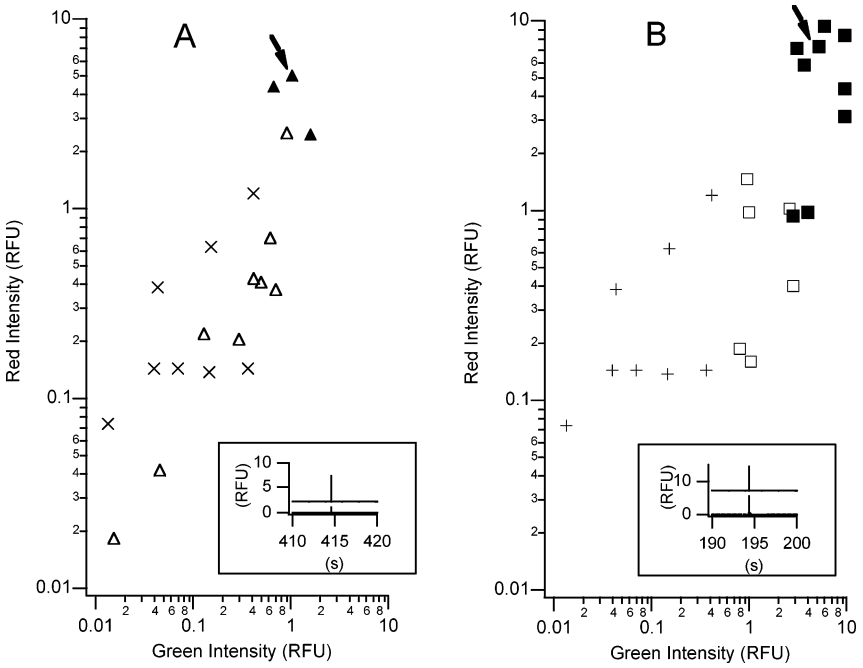

Figure 4. Red vs green signal intensities for the most intense event detected by single-cell CE-dual LIF. (A) Signal from cells expressing EGFP-KRS (open triangles), both EGFP-KRS and nuDsRed (solid triangles), or from untransfected cells (×'s). (B) Cells expressing EGFP-MRS (open squares), both EGFP-MRS and nuDsRed (solid squares), or from untransfected cells (crosses). The insets in panels A and B show the electropherogram for the data point indicated by an arrow. Upper and lower traces correspond to the red and green channels, respectively. The analytical conditions are the same as those described in Figure 3.

consistent with the microscopy data indicating that EGFP-MRS is localized in the nucleus.

In contrast, the average intensity of the narrow peak obtained from EGFP-KRS-expressing cells (0.41 ± 0.32 V, $n = 9$) is not significantly different (at a 95% confidence level) from that of the untransfected cells (0.16 ± 0.16 V, $n = 8$). Thus, it appears that the narrow peaks detected from EGFP-KRS cells (Figure 3C, trace II) are false positives due to autofluorescence. Thus, we conclude, based on these CE results, that EGFP-KRS is localized in the cytosol but is not present in the nucleus at levels that can be clearly differentiated from autofluorescence.

Dual-Channel Detection of EGFP-aaRS and nuDsRed. To further probe the nuclear localization of the EGFP-aaRS proteins, we carried out single-cell analyses using cells coexpressing one of the fusion proteins along with the nuclear marker nuDsRed. The dual-channel detection system (Figure 1) was used to detect the simultaneous localization of the two fluorophores within the same organelle.

Figure 4A shows a log−log plot of red versus green signal intensities for the most intense peak detected in both channels for untransfected cells (×'s), cells expressing EGFP-KRS only (open triangles), and cells expressing both EGFP-KRS and nuDsRed (solid triangles). The inset shows a representative electropherogram of a cell expressing both fusion proteins, with the signals in the red and green channels shown in the top and bottom traces, respectively. The red and the green intensities of the peaks resulting from both the untransfected and the EGFP-KRS cells are relatively low (i.e., <1 V). Furthermore, although the average green signal from EGFP-KRS cells (0.41 ± 0.32 V, $n = 9$) is larger than the signal from the untransfected cells (0.16 ± 0.16 V, $n = 8$), the data are not significantly different (at a 95% confidence level).

The most intense peak from cells expressing both fusion proteins (Figure 4A, solid triangles and inset) appears in the red channel (3.55 ± 1.32 V, $n = 3$), consistent with nuclear-localized nuDsRed. The corresponding peak in the green channel (inset, bottom trace) is similar in intensity to the most intense peaks from untransfected cells (×'s). Thus, these results support the conclusion that EGFP-KRS is localized in the cytosol but is not detectable in the nucleus.

We also analyzed single cells expressing both EGFP-MRS and nuDsRed using dual-channel detection. The inset of Figure 4B shows a representative electropherogram from such a cell. A high-intensity narrow peak (~194 s) is clearly detected simultaneously in the green channel (bottom trace) and the red channel (top trace), supporting nuclear localization of EGFP-MRS. Figure 4B is a log−log plot of red versus green signal intensities for the most intense peak detected in eight single untransfected cells (crosses), six cells expressing only EGFP-MRS (open squares), and nine cells expressing both EGFP-MRS and nuDsRed (solid squares). These data show that most of the peaks from cells expressing both EGFP-MRS and nuDsRed (solid squares) fall in the upper ranges of both red and green signal intensities. This distribution of signals is clearly distinguishable from autofluorescent peaks detected in untransfected cells (crosses) and supports the conclusion that EGFP-MRS is localized in the nucleus. The average intensity values are also consistent with this conclusion. The cells expressing both EGFP-MRS and nuDsRed have high green (5.93 ± 2.83 V, $n = 9$) and red (5.27 ± 3.11 V, $n = 9$) intensities. These values are significantly different from the green and red intensities from untransfected cells (0.16 ± 0.16 V and 0.36 ± 0.39 V, respectively, $n = 8$). Therefore, these peaks (solid squares) correspond to nuclei that are expressing both nuDsRed and EGFP-MRS. With the use of a recombinant EGFP standard (data not shown), the average amount of EGFP-MRS localized in the nucleus was determined to be ~5 zmol or 2% of the total EGFP-MRS content of a single cell. This percentage compares well with previous reports indicating that the nuclear aaRS content is ~2−3% for CHO cells and <1% for rabbit kidney cells.[4] Although the majority of peaks from the dual transfected cells have high red and green signals, two peaks have relatively low red fluorescence (Figure 4B). These peaks apparently correspond to EGFP-MRS-containing nuclei that have low levels of nuDsRed expression. Cell-to-cell variation in expression levels of proteins has been reported in previous single-cell CE studies.[28,31]

(31) Xue, Q.; Yeung, E. S. *J. Chromatogr., A* **1994**, *661*, 287−295.

CONCLUSIONS

In summary, CE-dual LIF was used to investigate the subcellular localization of fluorescent proteins in mammalian cells. In particular, to further probe the intriguing discovery of nuclear localization of aaRSs, human MRS and KRS were expressed as EGFP fusion proteins in human-derived ΔH2-1 osteosarcoma cells. With the use of fluorescence microscopy, both EGFP-aaRSs were detected in the cytosol, whereas only EGFP-MRS was clearly observed in the nucleus. The results of CE-LIF analysis of nuclei from single cells expressing only EGFP-MRS or EGFP-KRS were consistent with this conclusion. The CE method, which results in narrow peaks for proteins bound to an organelle and broad peaks for cytosolic proteins, offers several advantages over microscopy, including increased sensitivity and physical separation of cellular compartments.

Dual-channel CE-LIF was also used to probe aaRS cellular localization. The most intense peak in the green channel of single cells expressing both EGFP-KRS and nuDsRed did not show significant differences from autofluorescent signals, suggesting that EGFP-KRS is not found in the nuclei of ΔH2-1 cells (or its presence is obscured by nuclear autofluorescence). In contrast, single cells expressing both EGFP-MRS and nuDsRed showed simultaneous green and red narrow peaks that were easily distinguishable from autofluorescent peaks. This result indicated that EGFP-MRS is localized in the nuclei of ΔH2-1 cells. Taken together, these results demonstrate the feasibility of using CE-LIF as a new general method for determining the subcellular localization of proteins in single cells.

ACKNOWLEDGMENT

We thank Dr. Wongi Seol (Sung Kyun Kwan University, South Korea) for helpful discussions. ΔH2-1 cells are a gift from Dr. Carlos Moraes (Department of Neurology and Cell Biology & Anatomy, University of Miami, FL). Ms. Karen Olson's help in determining transfection efficiencies is appreciated. E.A. is supported through 1K02-AG21453. This work was supported by NIH Grants GM61969 (E.A.) and GM49928 (K.M.F.).

Received for review March 20, 2004. Accepted May 25, 2004.

AC049567E